JOURNAL OF GEOPHYSICAL RESEARCH, VOL. 111, B12S11, doi:10.1029/2006JB004562, 2006

Three-dimensional micromagnetic modeling of randomly oriented magnetite grains (0.03–0.3 μm)

Koji Fukuma[1] and David J. Dunlop[2]

Received 14 June 2006; revised 24 October 2006; accepted 7 November 2006; published 9 December 2006.

[1] We report three-dimensional micromagnetic structures obtained for magnetite cubes with ⟨100⟩ edges in the size range 0.03–0.3 μm around the single-domain threshold size. We employed the Metropolis algorithm to find equilibrium micromagnetic structures starting from uniformly magnetized initial states. Directions of initial magnetizations were randomly set so as to mimic a randomly oriented assemblage. Small grains (<0.07 μm) exhibit single-domain equilibrium structures parallel to a magnetic easy axis ⟨111⟩ irrespective of initial magnetization directions. Vortex structures emerge for small pseudosingle-domain grains above 0.07 μm. Axes of the vortices are parallel to ⟨100⟩ in the threshold size range but become randomly oriented with increasing grain size. Neither lamellar domain structures nor multiple vortex structures were found for grains smaller than 0.3 μm. Reduced saturation remanent magnetization decreased down to ~0.1 with increasing grain size over a relatively narrow grain size range (0.07–0.15 μm). The grain size variation of reduced magnetization depends on microscopic magnetization structures inside a single grain and the degree of randomness of grain magnetization directions in an assemblage.

Citation: Fukuma, K., and D. J. Dunlop (2006), Three-dimensional micromagnetic modeling of randomly oriented magnetite grains (0.03–0.3 μm), *J. Geophys. Res.*, *111*, B12S11, doi:10.1029/2006JB004562.

1. Introduction

[2] Magnetite grains in the transitional range between single-domain (SD) and pseudosingle-domain (PSD) are of paramount importance in paleomagnetism. Samples containing SD grains have high remanence intensity and stability and should reliably record the paleomagnetic field. However, the stable SD size range is very narrow or nonexistent for equant magnetite [*Newell and Merrill*, 1999]. Above the SD threshold size experimental data show a gradual rather than a sharp drop in remanence intensity and stability with increasing grain size [*Dunlop*, 1973], contrary to the prediction of classic domain theory. The term of PSD was coined for grains that exceed SD threshold size but exhibit high remanence and stability similar to SD [*Stacey*, 1962]. PSD grains, particularly those only slightly above SD threshold size, are likely to be dominant remanence carriers in natural samples in view of the narrow stable SD size range. The grain size dependence of magnetic properties is also useful for inferring the grain size of magnetic minerals in sediments used to detect environmental changes [*Thompson and Oldfield*, 1986; *Verosub and Roberts*, 1995].

[3] From the beginning of micromagnetic modeling the SD-PSD transitional range has been one of the prime targets. Many micromagnetic studies have examined how micromagnetic structures vary in response to changing grain size [e.g., *Williams and Dunlop*, 1989]. These studies have shown that the SD-PSD transition does not occur abruptly at a critical size dictated by the total free magnetic energy, contrary to the assumption of earlier nonmicromagnetic calculations [e.g., *Butler and Banerjee*, 1975]. However, the calculated magnetic intensities and stabilities drop rapidly in a relatively narrow size range above the SD threshold size (~0.07 μm) as determined from experimental results and nonmicromagnetic calculations [*Newell et al.*, 1993a; *Fabian et al.*, 1996; *Williams and Dunlop*, 1989]. Intriguing magnetic structures, such as vortex or flower structures [*Schabes and Bertram*, 1988], which are distinctively different from the classical structure of domains and domain walls, were found for the SD-PSD transitional range. At present, the SD-PSD transition is believed to be related to a structural transformation from a uniformly or almost uniformly magnetized state (single-domain, flower) to a vortex state with increasing grain size [*Williams and Wright*, 1998].

[4] In addition to microscopic magnetic structures, micromagnetic modeling can provide macroscopic magnetic properties that enable a direct comparison with experimental data. Several factors need to be considered before making such a comparison. The micromagnetic modeling for a single grain gives magnetic properties when an external magnetic field is applied at a particular angle to the crystallographic axis, whereas real assemblies of magnetic

[1]Department of Environmental System Science, Doshisha University, Kyotanabe, Japan.
[2]Geophysics, Physics Department, University of Toronto, Toronto, Ontario, Canada.

0148-0227/06/2006JB004562$09.00

grains contain a large number of randomly oriented grains. Therefore many grains with different orientations must be modeled to average out the dependence of magnetic properties on the angle between the field direction and the grain axes. Some of the micromagnetic calculations incorporated randomly oriented grains to simulate first-order reversal curve (FORC) diagrams [e.g., *Carvallo et al.*, 2006].

[5] Another problem is how we can obtain magnetic properties reflecting stable magnetic states. Micromagnetic calculations have been usually performed by starting from an arbitrarily chosen initial state and employing a conjugate gradient method to search for a final solution [e.g., *Williams and Dunlop*, 1989; *Newell and Merrill*, 2000a], although the Landau-Lifshitz-Gilbert equation is also used for micromagnetic calculations [e.g., *Muxworthy and Williams*, 2004; *Suess et al.*, 2002]. The conjugate gradient method locates the nearest local energy minimum (LEM) state but this is not necessarily a thermodynamically stable state. The system may remain trapped in a shallow minimum from which it would escape under real conditions with the aid of thermal energy. Since magnetic properties are measured at room temperature, it is unrealistic to ignore the effect of thermal fluctuations when making comparisons with experimental data.

[6] We have obtained three-dimensional micromagnetic structures of magnetite cubes over the size range from 0.03 to 0.3 μm, spanning the SD to PSD transition [*Butler and Banerjee*, 1975; *Newell and Merrill*, 2000b]. In order to simulate randomly oriented assemblies relative to the fixed direction of a uniform external field, initial states of individual grains are assigned to be uniformly magnetized (saturated) states with randomly chosen directions relative to the crystallographic axes. Sets of fifty such grains were calculated to average out the angular effect on magnetic properties. In order to find equilibrium structures, the magnetizations of each subcube were relaxed in zero field according to the Metropolis algorithm. This is a sort of Monte Carlo method that gives a thermodynamically equilibrium state and was proved to be effective in locating stable states in two-dimensional micromagnetic modeling [*Fukuma and Dunlop*, 1997, 1998] and is similar to a simulated annealing method adopted by *Thomson et al.* [1994].

2. Model

[7] Our model grain is a magnetite cube with edges along $\langle 100 \rangle$ axes that is one of typical crystal forms expected from its cubic symmetry [*Klein and Hurlbut*, 1993] (Figure 1). The $\langle 111 \rangle$ easy axes of magnetization lie along the body diagonals and the $\langle 100 \rangle$ edges are hard axes of magnetization. This coordinate system is the same as that adopted by *Williams and Dunlop* [1990] and *Fabian et al.* [1996]. Edge length is set in the range of 0.03 to 0.3 μm spanning SD-PSD boundary. The model cube was subdivided into $10 \times 10 \times 10$ subcubes to obtain its micromagnetic structure, so the spatial resolution is limited less than 0.03 μm or better even in the largest modeled grain, which is deduced from the size of magnetization swirl calculated as $3*(A/\mu_0 M_s^2)^{0.5}$ [*Hubert*, 1988], where A, μ_0 and M_s mean the exchange constant, the free-space magnetic permeability and the saturation magnetization, respectively. Such a cell size limit

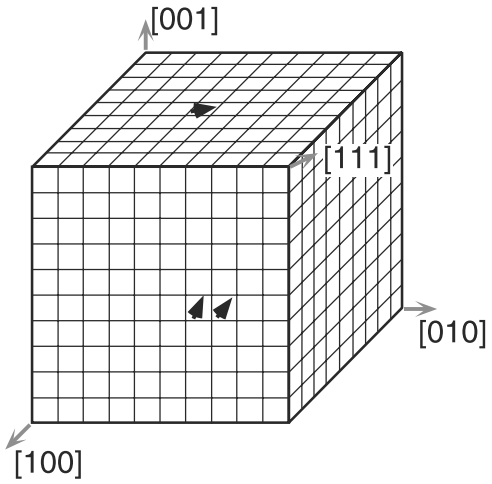

Figure 1. Model magnetite cube. Cube edges and body diagonals coincide with $\langle 100 \rangle$ hard axes and $\langle 111 \rangle$ easy axes of magnetization, respectively. The model cube is subdivided into $10 \times 10 \times 10$ subcubes to obtain micromagnetic structures.

of 0.03 μm was confirmed to be appropriate giving high values ($\sim$1) of the self-consistency parameter [*Newell et al.*, 1993a; *Fukuma and Dunlop*, 1998]. The magnetization of each subcube can rotate freely in three-dimensional space as part of a specified energy state.

[8] To obtain micromagnetic structures, we considered three magnetic free energy terms: exchange energy, magnetocrystalline anisotropy energy, and demagnetizing energy. Exchange energy E_e arises from interacting neighboring atomic spins. The assumption that spin directions vary gradually within a single subcube [*Brown*, 1978] leads to a following expression:

$$E_e = -Ad^3\Sigma(\boldsymbol{m}_i \cdot \Delta \boldsymbol{m}_i) \tag{1}$$

where A is the exchange constant and d and $\boldsymbol{m}_i$ are the edge length and the magnetization of a subcube. The Laplace operator Δ is replaced by a five-point difference approximation in our numerical calculation [*Labrune and Miltat*, 1990], which gives significantly smaller errors in calculating exchange energy [*Donahue and Porter*, 2004].

[9] Magnetocrystalline anisotropy energy E_a depends on the direction of each subcube magnetization relative to the crystallographic axes. For magnetite E_a is reasonably well expressed with the first-order term of the series expansion:

$$E_a = K_1 d^3 \Sigma\left(\alpha_1^2\alpha_2^2 + \alpha_2^2\alpha_3^2 + \alpha_3^2\alpha_1^2\right) \tag{2}$$

where K_1 is the anisotropy constant (negative) and α_1, α_2 and α_3 are the directional cosines of subcube magnetization with respect to the three $\langle 100 \rangle$ axes. The $\langle 100 \rangle$ edges of the model cube and the $\langle 111 \rangle$ body diagonals are hard and easy axes of magnetization, respectively. This definition of E_a was adopted in most previous three dimensional micromagnetic models [*Fabian et al.*, 1996; *Wright et al.*, 1997] and makes possible a direct comparison with their calculated energy values.

[10] Demagnetizing energy E_d, which originates from magnetostatic interactions between subcubes, is the computationally most intensive energy term. E_d is given by

$$E_d = \left(\mu_0 d^3 M_s^2/2\right)\Sigma\left(\boldsymbol{m}_i \cdot N_{ij}\boldsymbol{m}_j\right) \quad (3)$$

where N_{ij} is the demagnetizing tensor, which is defined by interactions of surface charges for pairs of subcubes i and j [*Rhodes and Rowlands*, 1954]. We developed N_{ij} for the three-dimensional calculations based on N_{ij} for the two-dimensional case [*Newell et al.*, 1993b]. We thoroughly checked the elements of the demagnetizing tensor given by *Wright et al.* [1997] with the aid of an algebra software "Mathematica" and found several discrepancies.

[11] In our modeling we assumed grains with no dislocations or other defects. Magnetoelastic energy was not considered and no magnetostrictive effects were included in the modeling. Such effects are certainly important for micron-sized magnetite or high-titanium titanomagnetite, but they do not affect magnetization states of magnetite less than 0.5 μm in size [*Fabian and Heider*, 1996]. Thus the total magnetic free energy E_t is given by the sum of the above three energy terms $E_t = E_e + E_a + E_d$.

[12] Final structures were obtained by following the Metropolis algorithm starting from an initially assigned structure. This algorithm was previously applied for two-dimensional micromagnetic modeling [*Fukuma and Dunlop*, 1997, 1998]. The magnetization vector in one subcube is rotated in a randomly chosen direction through an angle <5°. The rotation is accepted or rejected according to a transition probability W:

$$W = \begin{cases} 1 & \Delta E_t < 0 \\ \exp(-\Delta E_t/kT) & \Delta E_t > 0 \end{cases} \quad (4)$$

where ΔE_t is the consequent difference in total energy, k is Boltzmann's constant and T is absolute temperature. This means that if total energy decreases, the rotation is always accepted. Otherwise the rotation is accepted or rejected based on the probability calculated from the amount of increased total energy. Repeating such a trial rotation for each of the 1000 subcubes constitutes one Monte Carlo step (MCS). To achieve equilibrium states, as determined by no further reduction in total energy, such trial rotations needed to be repeated for several tens of thousands of MCS.

[13] To simulate a real assembly composed of randomly oriented grains, we obtained equilibrium states in the way just described for fifty identical grains when the external field was applied along randomly chosen directions within one octant of sphere. This calculation is equivalent to a calculation for 200 grains randomly oriented over a half sphere around a fixed field axis, which should be enough to average out angular effects between a crystallographic axis and an external field direction. Random directions in the octant were generated and statistically tested following *Fisher et al.* [1987] (Figure 2). The calculated mean direction is statistically indistinguishable from the expected mean direction [111].

[14] In the modeling, each initial structure was a saturated state, although initial vortex structures were also given for comparison. Thus the initial magnetizations of all subcubes were placed in randomly chosen directions and then a final equilibrium state was sought following the Metropolis algorithm. The saturation remanence M_{rs} for a given grain size was calculated by vectorially summing the final magnetization of all 50 grains relative to a field axis fixed in space. These calculated values of M_{rs} can be directly compared with experimental data, unlike previous modelings with a limited number of results calculated in a few particular directions [*Williams and Dunlop*, 1995].

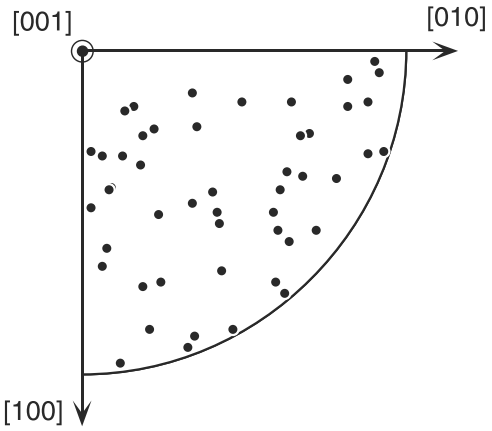

Figure 2. Equal-area plot of randomly oriented initial magnetization directions as viewed from the crystallographic orientation of each grain.

[15] We used magnetic parameters of magnetite at room temperature T = 298 K, namely $M_s = 4.80 \times 10^5$ A/m, $A = 1.32 \times 10^{-11}$ J/m^3, $K_1 = -1.25 \times 10^4$ J/m^3. The computation required about 10 hours for 50 grains of a particular grain size using a NEC SX4 parallel-vector computer with 32 processors and a shared memory.

3. Results

[16] We found several characteristic micromagnetic structures in the SD-PSD transition range starting from initial saturated states for randomly oriented assemblages. In order to examine the effect of initial states, calculations were also performed starting from initial vortex structures. There was no discrepancy in the final structures when started from saturated or vortex states. They end up in the same final SD or vortex structures depending on a given grain size. In order to reveal the interior structure, the illustrations show three views in slices parallel to the x-y planes in addition to the surface structure (Figure 3).

[17] Effectively single-domain structures along the [111] easy magnetization axis emerge irrespective of the initial magnetization directions for grains smaller than 0.06 μm (Figures 3a and 4a). This result implies that magnetocrystalline anisotropy controls the magnetization direction. However, the magnetization vectors of subcubes are not completely parallel to each other and randomly and slightly deviate from [111], lowering the ratio of saturation remanence to saturation magnetization (M_{rs}/M_s) less than unity and giving rise to high exchange energy (Figure 5). This nonparallelism is due to thermal fluctuations, which are incorporated in our model but were not considered in previous models [*Newell and Merrill*, 2000b]. Flower structures, in which magnetizations are almost uniform in direction but systematically and slightly deviate from neigh-

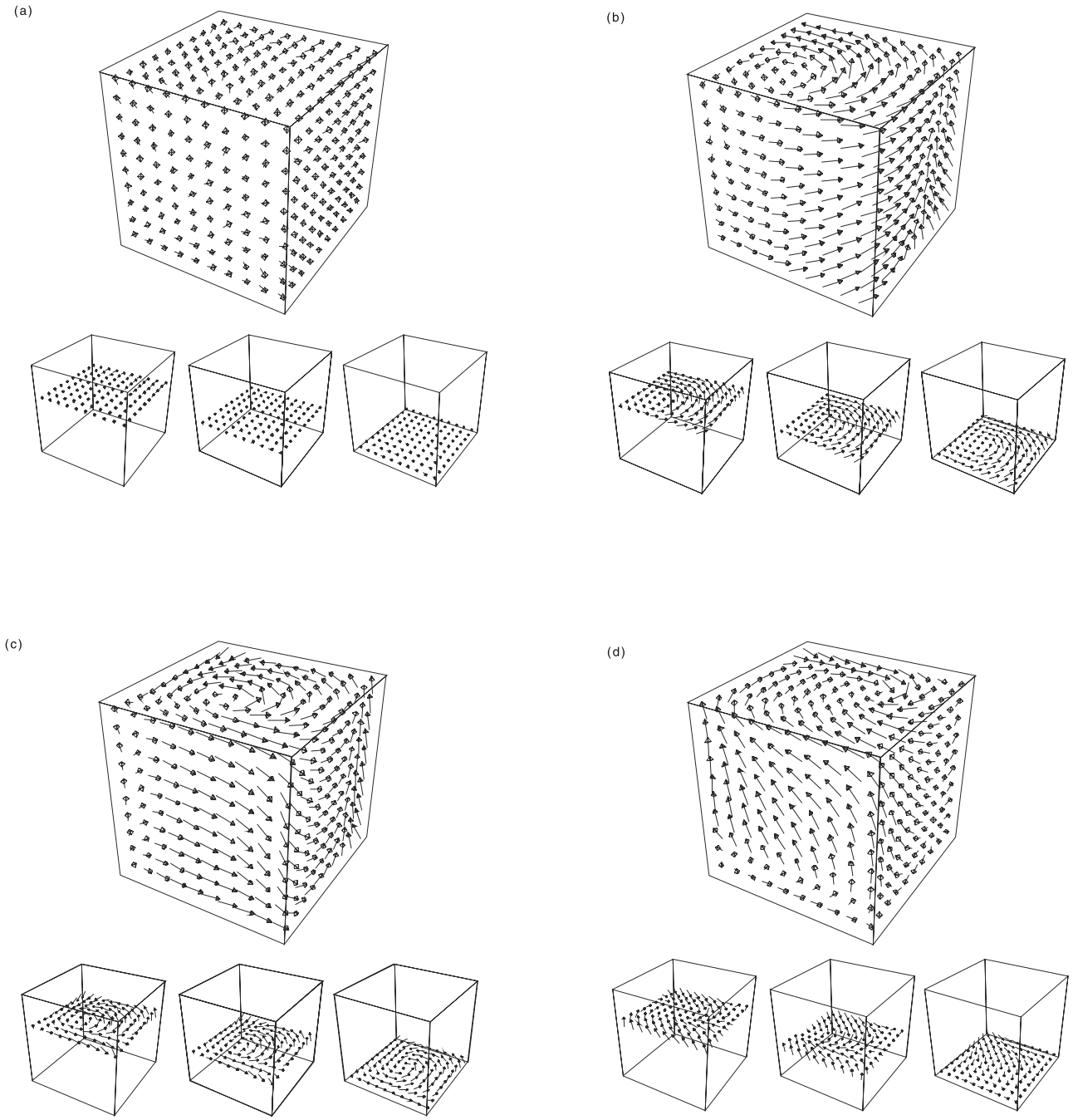

Figure 3. Equilibrium magnetization structures for SD and PSD grains: (a) 0.05 μm, (b) 0.09 μm, and (c) and (d) 0.25 μm. Surface and interior magnetization patterns are shown to illustrate the three-dimensional structure. Each vector represents the magnetization of one subcube.

boring ones, were not found in our calculations, although they have been reported previously starting from initial saturated states [*Schabes and Bertram*, 1988; *Williams and Wright*, 1998; *Fabian et al.*, 1996]. *Williams and Wright* [1998] found a flower structure whose net magnetization is parallel to a $\langle 001 \rangle$ edge, and suggested that demagnetizing energy controls the magnetization direction. In our calculations, however, even if started from an initial magnetization parallel to the $\langle 001 \rangle$ axes, the equilibrium magnetization became parallel to a $\langle 111 \rangle$ direction (Figure 4a).

[18] Vortex structures emerge for grains larger than 0.07 μm and up to 0.3 μm, which is the maximum size considered in this study (Figure 3b). The axis of the vortex is parallel to a $\langle 100 \rangle$ edge of the cube and the magnetization vectors near the edges are aligned along the edge directions (Figure 4b). Such a vortex structure was found in previous three-dimensional modeling from an initial quasi-vortex structure [*Williams and Wright*, 1998; *Fabian et al.*, 1996] and in a two-dimensional modeling starting from a saturated state [*Fukuma and Dunlop*, 1998]. Since curling microscopic magnetizations cancel one another in the plane of

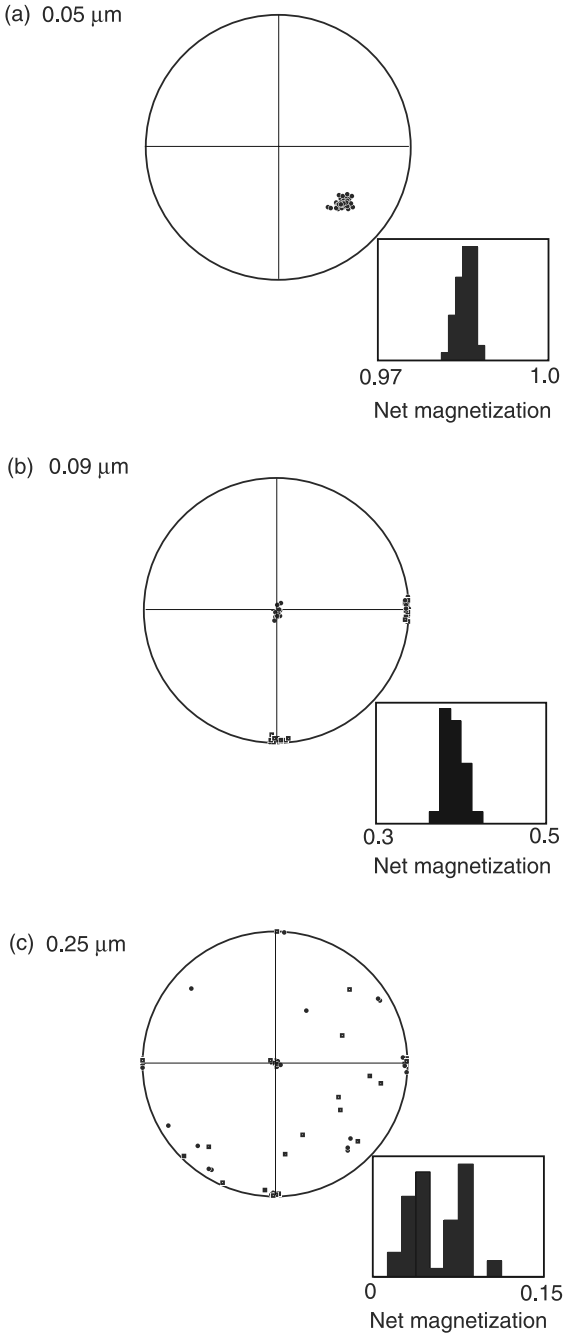

Figure 4. Equal-area projections of magnetization directions of equilibrium states and histograms of normalized net magnetization values for (a) 0.05 μm, (b) 0.09 μm, and (c) 0.25 μm grains.

curling, the net magnetization of the vortex structure is parallel to one of the $\langle 100 \rangle$ axes. The net magnetization arises both from the vortex axis and from the edge magnetizations (Figure 3b). Starting from various initial directions, the final directions fall in the nearest $\langle 100 \rangle$ axis (Figure 4b). There is a superficial resemblance to the magnetization of a SD grain with cubic anisotropy and $K_1 > 0$, such as iron. However, here the final magnetic structure is vortex with a much lower remanence than SD.

[19] With further increase in grain size, the magnetization structure becomes more complicated, although essentially it remains a vortex structure. In smaller grains, the magnetizations of the vortex axis and the edges are parallel and in the same sense (Figure 3b), giving rise to a comparatively high net magnetization ($\sim$0.4 for 0.09 μm grains). In larger grains, as shown for a 0.25 μm grain in Figure 3c the edge magnetizations have opposite senses and are mutually canceling. The net magnetization is much lower (0.048) compared to smaller grains exhibiting a vortex structure (Figure 3b), although the overall structure is not greatly changed. This means that even within vortex structures, the net magnetization is variable depending on microscopic features such as the directions of the edge magnetizations.

[20] Another type of structure was found for the identical grain size 0.25 μm (Figure 3d), although it is still similar to

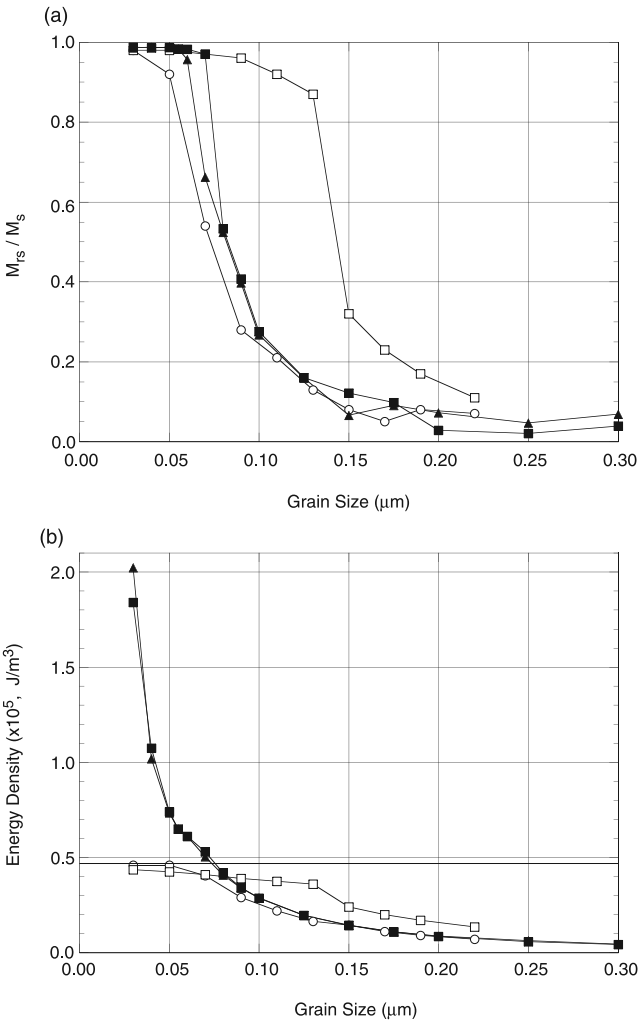

Figure 5. Grain size dependence of (a) M_{rs}/M_s and (b) energy density of equilibrium states for two extreme cases: initially magnetized along a [100] hard axis and along a [111] easy axis. For comparison, the results for a magnetite cube [*Fabian et al.*, 1996] calculated by a conjugate gradient method are shown. Solid square and triangle indicate initial magnetization along [111] and [100] (this study); open square and circle indicate initial [111] SD and vortex states [*Fabian et al.*, 1996]. A horizontal line in Figure 5b represents the energy density value of completely aligned magnetizations of single-domain state.

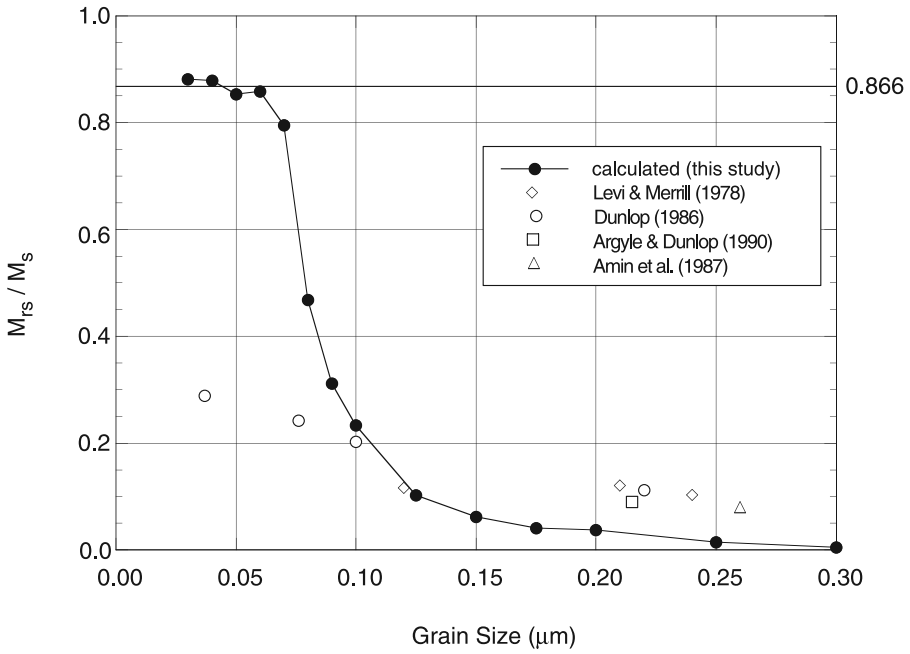

Figure 6. Comparison of calculated M_{rs}/M_s for randomly oriented assemblages (solid circles) and experimental data on sized synthetic magnetites (open symbols) [*Levi and Merrill*, 1978; *Dunlop*, 1986; *Amin et al.*, 1987; *Argyle and Dunlop*, 1990]. The expected value of M_{rs}/M_s (0.866) for a single-domain magnetite governed by magnetocrystalline anisotropy is shown by a horizontal line.

a vortex structure. At the top surface, the magnetization makes a single curling, very similar to the vortex structure of the same size grain (Figure 3c). However, the magnetization gradually become uncurls downward and no curling is observed at the bottom plane. A vortex occupies only the upper part of the cube, and such a three-dimensional feature cannot be represented even approximately with two-dimensional modeling. This kind of structure may correspond to a twisted vortex structure found for larger grains that also show simple vortex structures [*Rave et al.*, 1998]. The net magnetization is larger than that of a vortex structure and is largely deflected from the [001] vortex axis of the upper part of the cube. Grains of the same size split into two types of magnetization structures depending on the initial directions of magnetization, and the final net magnetization values have a bimodal distribution (Figure 4c).

[21] In order to make a direct comparison with previous modeling results, we showed the grain size dependence of net magnetization when starting from initial [111] and [001] saturated states (Figure 5). *Fabian et al.* [1996] started their calculations with initial [111] saturated states and initial single-vortex states. They obtained quite different evolution trends with grain size for these two families. Our results for the [111] family are directly comparable to those of Fabian et al.'s [111] family but give much lower net magnetization values above 0.08 μm (Figure 5), where we find essentially no uniform structure. Our [111] trend is rather similar to their single-vortex trend and our [001] trend. This is because vortex structures emerge when calculations are started from initial saturated states for grains larger than 0.08 μm (Figure 3b).

[22] *Fabian et al.* [1996] reported that their [111] family of states evolves from a flower to a double-vortex structure between 0.13 and 0.15 μm. Also energy states for double vortex structures were mapped out using a constrained calculation [*Muxworthy et al.*, 2003]. In our modeling, however, neither of these structures emerges for the same family based on the Metropolis algorithm. Our energy density for the [111] family of states also drops below theirs around 0.08 μm (Figure 5b), although below 0.08 μm we obtained higher energy density due to enhanced exchange energy resulting from nonparallel neighboring magnetizations induced by thermal fluctuations (Figure 3a). Thus vortex structures are lower energy states, i.e., more stable states, above 0.08 μm than flower or double-vortex states. Our interpretation is that Fabian et al.'s calculations stalled in higher energy LEM states between 0.08 and 0.15 μm. With thermal energy, the system can escape to lower energy single-vortex states.

[23] The evolution trend with grain size for initial [001] states is not greatly different from that of initial [111] states (Figure 5a). In the SD size range, these results give high net magnetization, close to unity, of completely aligned subcube magnetizations, irrespective of initial directions. A notable difference is that the [100] trend shows a much lower net magnetization than the [111] trend around 0.07 μm (Figure 5), which is in the transitional range from SD to vortex structure. The initial [111] saturated state results in a [111] single-domain structure with a still high value ($\sim$0.97) of net magnetization, whereas a vortex structure with an [100] axis results from the initial [100] saturated state and has a considerably lower value ($\sim$0.67) of net magnetization.

[24] In order to compare with experimental data, we calculated ratios of saturation remanence to saturation magnetization (M_{rs}/M_s) for randomly oriented assemblages by vectorially summing the net magnetizations of the 50 grains of each size (Figure 6). For SD grains, the calculated value is close to the expected value 0.866 calculated

analytically for grains with cubic anisotropy and [111] easy axes. Above 0.06 μm, M_{rs}/M_s decreases rapidly down to about 0.1 for 0.125 μm grains, resembling the net magnetization variation for [001] and [111] initial directions (Figure 5a). Such a rapid change of M_{rs}/M_s basically results from the transformation from SD to vortex structure of each grain. The relative proportions of SD and vortex structures for a particular grain size (e.g., 0.07 μm as discussed above) and the axis and edge magnetizations of a particular vortex structure basically determine the grain size dependence of M_{rs}/M_s of the randomly oriented assemblage. Grains larger than 0.15 μm still show a systematic decrease of M_{rs}/M_s with increasing grain size, although the net magnetization of a particular family does not show any systematic dependence (Figure 5a). Such a decrease of M_{rs}/M_s can be attributed to the fact that net magnetization directions become more scattered with increasing grain size (Figure 4).

4. Discussion

[25] The critical grain size at which the SD state in cubic magnetite begins to destabilize is estimated to be 0.07 μm in our three-dimensional micromagnetic modeling for randomly oriented grains (Figures 5 and 6). This critical size estimate agrees with values reported in previous two- or three-dimensional modelings [e.g., *Newell et al.*, 1993a; *Fabian et al.*, 1996; *Williams and Wright*, 1998; *Witt et al.*, 2005]. Even classical nonmicromagnetic modeling assuming lamellar domain structures gives a similar critical size [*Butler and Banerjee*, 1975] and this calculated value is frequently cited as supporting evidence for fossil biogenic magnetite of SD size [e.g., *Thomas-Keprta et al.*, 2000]. Our modeling, which includes the effects of thermal fluctuations and random grain orientations, still reproduces essentially the same SD critical size. This means that the critical SD size is insensitive to specific features of micromagnetic models and that previous models provided a reliable estimate of the critical SD grain size. These numerically calculated results are supported by an analytical solution giving a critical SD size of 0.06 μm, which is not far above the superparamagnetic threshold size [*Newell and Merrill*, 1999].

[26] Above the critical SD size ($\sim$0.07 μm), saturation remanence does not suddenly drop to zero but it does decrease rapidly with increasing grain size (Figures 5 and 6). This is one of the prominent experimental indicators of PSD effects in magnetite. Micromagnetic states in this transitional size range are represented by a single-vortex structure in which the curling of magnetization occupies the entire grain and the curling axis parallels the $\langle 100 \rangle$ cube edge. In most cases, SD and single-vortex states do not coexist in grains of the same size, irrespective of the initial states. This finding disagrees with previous micromagnetic results showing a broad size range of coexisting SD (or flower) and single-vortex structures up to 0.2 μm [*Fabian et al.*, 1996; *Williams and Wright*, 1998].

[27] Depending on initial states, metastable SD grains with higher free energy in principle still exist, but these SD grains are in shallow LEM states and do not represent actual structures found in nature, as our thermal fluctuation simulations demonstrate. Although coexisting SD and vortex structures are able to explain large magnetization values in the SD-PSD transitional range, this coexistence does not seems plausible because possibly there low-energy transition paths exist between the two states. In single-vortex structures, the volume fraction occupied by the vortex axis decreases with increasing grain size. Magnetization arising from the vortex axis contributes to nonzero but rapidly decreasing magnetization in the transitional range slightly above the SD-PSD boundary.

[28] We computed structures of 50 randomly oriented grains for a single grain size. This modeling provides calculated values that can be directly compared with experimental data for synthetic samples containing randomly oriented grains. A rapid change in saturation remanence near the critical SD size (0.07 μm) can be seen both in experimental and calculated data (Figure 6). Our results predict a very high saturation remanence values ($\sim$0.866, as expected for grains with a cubic magnetocrystalline anisotropy), whereas the experimental values for SD grains are much lower, $\sim$0.3 [*Dunlop*, 1986]. Such low experimental values may reflect a dominant uniaxial shape anisotropy and contamination of superparamagnetic or PSD grains. Above 0.20 μm, the experimental values of saturation remanence are higher than predicted ($\sim$0.1) and show very weak grain size dependence. Contrary to the experimental data, our calculated results predict a continuous decrease with grain size. It should be noted that in this modeling, we did not include magnetoelastic effects that might be significant in controlling magnetization processes in this size range [*Fabian and Heider*, 1996].

[29] A sequence of SD, single-vortex, twisted-vortex and closure domain states was generally found for magnetic grains with uniaxial anisotropy of various magnitude [*Rave et al.*, 1998]. Although magnetite has cubic anisotropy with a relatively small negative anisotropy constant K_1, a similar sequence is expected for SD-PSD magnetites. SD converts to a single-vortex structure at about 0.07 μm and the interior structure of the vortex becomes more complicated as the grain size increases (Figure 3). Such complicated structures may be analogous to twisted-vortex structures for uniaxial anisotropy grains. *Fukuma and Dunlop* [1998] obtained a chaotic structure in two-dimensional micromagnetic modeling of 0.4 μm grains, suggesting that the actual structure would be too complicated to be represented in two dimensions. Above 0.7 μm, closure domain structures with three body domains persist at least up to 2.5 μm in the two-dimensional modeling. PSD effects of magnetite would plausibly originate from a micromagnetic structural transformation from SD to closure domain structure through varying vortex structures.

5. Conclusions

[30] Three-dimensional micromagnetic results for randomly oriented grains between 0.03 and 0.3 μm show a transformation from SD to vortex structures with increasing grain size. No metastable SD, flower or double-vortex states were found as equilibrium saturation remanence states. The SD to vortex change occurs around 0.07 μm, which corresponds to previously reported SD critical size estimates, and explains the observed noncritical but rapid change of saturation remanence just above the SD threshold size. The relatively high magnetization of these small PSD

grains, originating from vortex axis and edge magnetizations, and the varying volumetric fraction of the vortex axis region with grain size lead to a continuous grain size dependence of saturation remanence. Above 0.15 μm, vortex structures become more complicated and grain magnetization directions are more scattered. These effects contribute to the further slow but continuing decrease of magnetization with grain size.

[31] **Acknowledgments.** This paper was substantially improved by critical reviews from Ron Merrill and an anonymous reviewer. This research has been supported by NSERC Canada grant A7709 to D.J.D.

References

Amin, N., S. Arajs, and E. Matijevic (1987), Magnetic properties of uniform spherical magnetite particles from ferrous hydroxide gels, *Phys. Status Solids A*, *101*, 233–238.

Argyle, K. S., and D. J. Dunlop (1990), Low-temperature and high-temperature hysteresis of small multidomain magnetites (215–540 nm), *J. Geophys. Res.*, *95*, 7069–7083.

Brown, W. F. (1978), *Micromagnetics*, 143 pp., Krieger, New York.

Butler, R. F., and S. K. Banerjee (1975), Theoretical single-domain grain size range in magnetite and titanomagnetite, *J. Geophys. Res.*, *80*, 4049–4058.

Carvallo, C., A. R. Muxworthy, and D. J. Dunlop (2006), First-order reversal curve (FORC) diagrams of magnetic mixtures: micromagnetic models and measurements, *Phys. Earth Planet. Inter.*, *154*, 308–322.

Donahue, M. J., and D. G. Porter (2004), Exchange energy formulations for 3D micromagnetics, *Physica B*, *343*, 177–183.

Dunlop, D. J. (1973), Superparamagnetic and single-domain threshold sizes in magnetite, *J. Geophys. Res.*, *78*, 1780–1793.

Dunlop, D. J. (1986), Coercive force and coercivity spectra of submicron magnetites, *Earth Planet. Sci. Lett.*, *78*, 288–295.

Fabian, K., and F. Heider (1996), How to include magnetostriction in micromagnetic models of titanomagnetite grains, *Geophys. Res. Lett.*, *23*, 2839–2842.

Fabian, K., A. Kirchner, W. Williams, F. Heider, T. Leibl, and A. Hubert (1996), Three-dimensional micromagnetic calculations for magnetite using FFT, *Geophys. J. Int.*, *124*, 89–104.

Fisher, N. I., T. Lewis, and B. J. J. Embleton (1987), *Statistical Analysis of Spherical Data*, 329 pp., Cambridge Univ. Press, New York.

Fukuma, K., and D. J. Dunlop (1997), Monte Carlo simulation of two-dimensional domain structures in magnetite, *J. Geophys. Res.*, *102*, 5135–5143.

Fukuma, K., and D. J. Dunlop (1998), Grain size dependence of two-dimensional micromagnetic structures for pseudo-single-domain magnetite (0.2–2.5 μm), *Geophys. J. Int.*, *134*, 843–848.

Hubert, A. (1988), The role of 'magnetization swirls' in soft magnetic materials, *J. Phys.*, *49*, 1859–1864.

Klein, C., and C. S. Hurlbut Jr. (1993), *Manual of Mineralogy*, 21st ed., John Wiley, Hoboken, N. J.

Labrune, M., and J. Miltat (1990), Micromagnetics of strong stripe domains in NiCo thin films, *IEEE Trans. Magn.*, *40*, 2450–2458.

Levi, S., and R. T. Merrill (1978), Properties of single-domain, pseudo-single-domain and multidomain magnetite, *J. Geophys. Res.*, *83*, 309–323.

Muxworthy, A. R., and W. Williams (2004), Distribution anisotropy: the influence of magnetic interactions on the anisotropy of magnetic remanence, in *Magnetic Fabric: Methods and Applications*, edited by F. Martín-Hernández et al., *Geol. Soc. Spec. Publ.*, *238*, 37–47.

Muxworthy, A. R., D. J. Dunlop, and W. Williams (2003), High-temperature magnetic stability of small magnetite particles, *J. Geophys. Res.*, *108*(B5), 2281, doi:10.1029/2002JB002195.

Newell, A. J., and R. T. Merrill (1999), Single-domain critical sizes for coercivity and remanence, *J. Geophys. Res.*, *104*, 617–628.

Newell, A. J., and R. T. Merrill (2000a), Nucleation and stability of ferromagnetic states, *J. Geophys. Res.*, *105*, 19,377–19,391.

Newell, A. J., and R. T. Merrill (2000b), Size dependence of hysteresis properties of small pseudo-single-domain grains, *J. Geophys. Res.*, *105*, 19,393–19,403.

Newell, A. J., D. J. Dunlop, and W. Williams (1993a), A two-dimensional micromagnetic model of magnetizations and fields in magnetite, *J. Geophys. Res.*, *98*, 9533–9549.

Newell, A. J., W. Williams, and D. J. Dunlop (1993b), A generalization of the demagnetizing tensor for nonuniform magnetization, *J. Geophys. Res.*, *98*, 9551–9555.

Rave, W., K. Fabian, and A. Hubert (1998), Magnetic states of small cubic particles with uniaxial anisotropy, *J. Magn. Magn. Mater.*, *190*, 332–348.

Rhodes, P., and G. Rowlands (1954), Demagnetizing energies of uniformly magnetized rectangular blocks, *Proc. Leeds Philos. Lit. Soc. Sci. Sect.*, *6*, 191–210.

Schabes, M. E., and H. N. Bertram (1988), Magnetization processes in ferromagnetic cubes, *J. Appl. Phys.*, *64*, 1347–1357.

Stacey, F. D. (1962), A generalized theory of thermoremanence, covering the transition from single-domain to multi-domain magnetic grains, *Philo. Mag.*, *7*, 1887–1900.

Suess, D., V. Tsiantos, T. Schrefl, J. Fidler, W. Scholz, H. Forster, R. Dittrich, and J. Miles (2002), Time resolved micromagnetics using a preconditioned time integration method, *J. Magn. Magn. Mater.*, *248*, 298–311.

Thomas-Keprta, K. L., D. A. Bazylinski, J. L. Kirschvink, S. J. Clement, D. S. McKay, S. J. Wentworth, H. Vali, E. K. Gibson Jr., and C. S. Romanek (2000), Elongated prismatic magnetite crystals in ALH84001 carbonate globules: Potential Martian magnetofossils, *Geochim. Cosmochim. Acta*, *64*, 4049–4081.

Thompson, R., and F. Oldfield (1986), *Environmental Magnetism*, 227 pp., Allen and Unwin, London.

Thomson, L., R. J. Enkin, and W. Williams (1994), Simulated annealing of three-dimensional micromagnetic structures and simulated thermoremanent magnetization, *J. Geophys. Res.*, *99*, 603–609.

Verosub, K. L., and A. P. Roberts (1995), Environmental magnetism: Past, present and future, *J. Geophys. Res.*, *100*, 2175–2192.

Williams, W., and D. J. Dunlop (1989), Three-dimensional micromagnetic modeling of ferromagnetic domain structure, *Nature*, *337*, 634–637.

Williams, W., and D. J. Dunlop (1990), Some effects of grain shape and varying external magnetic fields on the magnetic structure of small grains of magnetite, *Phys. Earth Planet. Inter.*, *65*, 1–14.

Williams, W., and D. J. Dunlop (1995), Simulation of magnetic hysteresis in pseudo-single-domain grains of magnetite, *J. Geophys. Res.*, *100*, 3859–3871.

Williams, W., and T. M. Wright (1998), High-resolution micromagnetic models of fine grains of magnetite, *J. Geophys. Res.*, *103*, 30,537–30,550.

Witt, A., K. Fabian, and U. Bleil (2005), Three-dimensional micromagnetic calculations for naturally shaped magnetite: Octahedra and magnetosomes, *Earth Planet. Sci. Lett.*, *233*, 311–324.

Wright, T. M., W. Williams, and D. J. Dunlop (1997), An improved algorithm for micromagnetics, *J. Geophys. Res.*, *102*, 12,085–12,094.

D. J. Dunlop, Geophysics, Physics Department, University of Toronto, Toronto, ON, Canada M5S 1A7.

K. Fukuma, Department of Environmental System Science, Doshisha University, Kyotanabe, 610-0394 Japan. (kfukuma@mail.doshisha.ac.jp)